

Usage of 3D prints with ceramic coating applied as neurological tools - preliminary research

Arkadiusz Szarek^{1*}, Justyna Łukomska- Szarek², Grzegorz Stradomski³, Maciej Nadolski³,
Wojciech Wolański⁴, Kamil Joszko⁴, Katarzyna Nowakowska-Langier⁵, Sebastian Okrasa⁵,
Dawid Larysz^{6,7}, Patrycja Larysz⁷

¹ Department of Technology and Automation, Faculty of Mechanical Engineering and Computer Science,
Czestochowa University of Technology, Częstochowa, Poland;

² Faculty of Management, Czestochowa University of Technology, Częstochowa, Poland;

³ Faculty of Production Engineering and Materials Technology, Czestochowa University of Technology,
Częstochowa, Poland;

⁴ Department of Biomechanics, Faculty of Biomedical Engineering, Silesian University of Technology, Zabrze,
Poland;

⁵ National Centre for Nuclear Research, Material Physics Department, Otwock-Swierk, Poland;

⁶ Department of Head and Neck Surgery for Children and Adolescents, University of Warmia and Mazury in
Olsztyn, Olsztyn, Poland;

⁷ Department of Head and Neck Surgery for Children and Adolescents, Prof. St. Popowski Regional Specialized
Children's Hospital, Olsztyn, Poland;

*Correspondence: Arkadiusz Szarek, Department of Technology and Automation, Faculty of Mechanical
Engineering and Computer Science, Czestochowa University of Technology, 42-201 Czestochowa, Poland; e-mail
address: arkadiusz.szarek@pcz.pl

Submitted: 31st January 2024

Accepted: 16th April 2024

Abstract:

Purpose: The paper shows a preliminary study of the basic strength parameters of printed parts made of biocompatible polymers with ceramic layers applied to increase the strength of the tool cutting surface.

Methods: The specimens were made from different materials and using different 3D printing technologies and the working surfaces that will eventually form the cutting element of the tool were coated with Al₂O₃. Gloss tests were conducted, properties of the coating, a scratch test of the coated surface, also evaluated surface topography.

Results: Based on the conducted research, it was found that polymeric materials are characterized by sufficient strength and can be used for disposable tools, however, the use of thin layers of Al₂O₃ significantly increases the surface strength parameters, which may have a significant impact on the reliability and durability of the tools. The polymer surface covered with an Al₂O₃ layer is characterised by increased scratch resistance ranging from 24% to 75% depending on the core material and printing technology. The gloss of the surfaces is disproportionately low compared to currently used metal tools, which indicates that they can be used in endoscopic procedures.

Conclusions: Based on the conducted research, it was found that the use of thin layers of Al₂O₃ covering polymer 3D prints is an excellent way to increase strength parameters such as scratch resistance, tribological parameters, and light reflections arising on the surface as a result of endoscopic lighting are disproportionately small compared to metallic biomaterials. This gives great hope for using polymer 3D prints for personalised neurosurgical tools.

Keywords: 3D printing, DLP, Digital Light Processing, FDM, FFF, light-cure resin, scratch test, neurosurgical instruments

1. Introduction

Minimally invasive neurosurgical procedures applied in the treatment of neonates with rare craniofacial congenital anomalies are the most important procedures in modern craniofacial surgery. Personalised distraction osteogenesis procedures, especially made with endoscopic assist allow very early, more effective and minimal-risk treatment The biggest advantage is to preserve large intracranial vessels which are part of the dura–dural sinuses. These blood vessels, i.e. superior sagittal sinus, transverse sinuses and sigmoid sinuses are strictly connected to the bones of the

skull. During surgery, the bones are cut and reconstructed. The crucial points are the detachment of the dura and its sinuses from the bones and the cutting just above the vessels. Bleeding from dural sinuses, especially in neonates or small children is potentially fatal. That's why the greatest effort should be made to make the preparation as safe and precise as much as it is possible. In Figure 1. examples of preoperative planning of the aforementioned procedures are presented. Conventional instruments made of metal alloys are used in neurosurgical operations, as lasers cannot be used to prevent thermal obliteration of blood vessels and damage to nerve tissue. The production of individualized metal alloy tools is a long-term and uneconomic process. Therefore, an attempt was made to develop ultra-modern polymer prints coated with hard ceramic layers to enable the manufacturing of personalized neurosurgical instruments with complex shapes and enhanced surface strength parameters to enable minimally invasive endoscopic procedures (see Fig. 1).

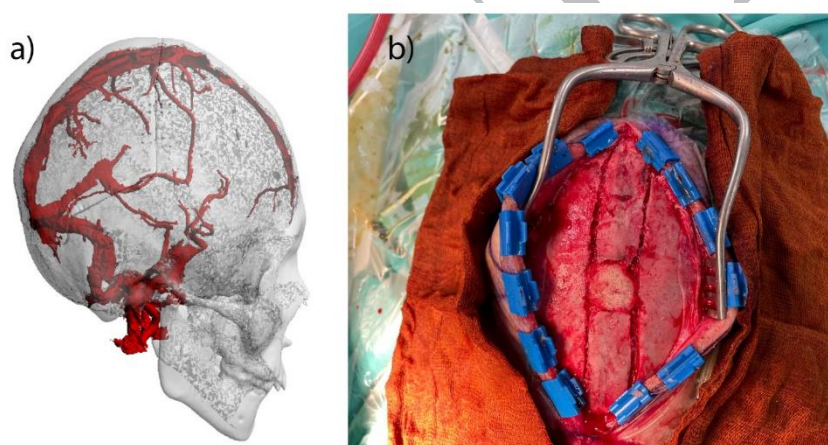


Fig. 1. Personalized neurosurgical procedures: (a) 3D CT reconstruction. Note the red large venous sinuses that are strictly connected to the bones, (b) intraoperative image of a minimally invasive neuroendoscopic surgery.

3D printing technologies involve manufacturing of complex geometric shapes using layer-by-layer application of material, resulting in a finished product in a relatively short period. Currently, the growing popularity of this manufacturing method is determined by the increasing availability of equipment, lower costs throughout the production cycle, and the possibility of obtaining precise parts with complex shapes, often extremely difficult to obtain using conventional manufacturing methods such as injection moulding, casting, or machining. Combining different manufacturing techniques opens up new opportunities for the development of incremental technologies [8, 9, 22].

The increasingly new material resources, including certified medical biomaterials, open up new possibilities for the use of this technology in various medical fields, although it should be taken into account that the strength parameters of polymeric bioprints still leave much to be desired [21]. A wide variety of components, including surgical instruments, implants, and bone screw guides, are now being made using the 3D printing method. All of these components must be thoroughly tested for biocompatibility and both mechanical and chemical strength. Research and testing are still underway to improve printed medical devices to make them as safe as possible for patients and facilitate recovery after surgical procedures [5, 25, 28].

Modifications to 3D-printed product surfaces are now a very popular area of interest for researchers. Improved tribological properties of prints, better quality of the surfaces, and reduction in the proliferation of microorganisms are very important fields of modern science [3, 15].

The purpose of the presented research was to determine the cohesive properties of Al₂O₃ coatings applied to 3D prints made using FDM (Fused Deposition Modeling) technology from copper-doped PLA (polylactide) and polyethylene terephthalate (PET) materials, and using DLP (Digital Light Processing) technology from two types of light-curing resins. The studies are being carried out with a team of neurosurgeons and provide the basis for the development of a procedure and technology to manufacture personalized neurosurgical tools with improved strength compared to polymer tools. By defining the requirements for the tools, the scope of examinations was defined to determine the optimal material strength and layer cohesion and to determine the gloss that hinders the endoscopic procedure. The article also evaluated the surface profiles of the 3D prints before and after the application of the coating, as in numerous neurosurgical procedures, very high accuracy of the cutting surface is required due to the large vascularization and innervation of the brain.

2. Materials and Methods

The tests were conducted on standard samples for pin-on-disc testing made on a 3D printer using fused deposition modelling from filaments designed for contact with human tissue and digital light processing from light-curable methacrylate resins. The materials used to make the specimens were: (1) specimen 1: PLA filaments with 3% copper addition, (2) specimen 2: PET-G filaments and resins designed for the manufacture of intraoral dental models, as well as a resin used for implant stencils. Specimens after the 3D printing process were prepared for further processing by removing

any supporting materials and rafts. For DLP prints, the materials used were (1) specimen 3: a light-curing resin for the production of dental drill guides, and (2) specimen 4: a light-curing resin for the production of dental models for orthodontics and prosthodontics. After printing, the specimens were thoroughly cleaned of any residual liquid material and additional curing was performed in a UV lamp. The next step was to apply the Al₂O₃ coating to the properly prepared surfaces of the specimens. The finished coated specimens were subjected to microscopic examination, evaluation of surface topography, and cohesion of the ceramic layer to the polymer core. The cohesion test consisted of scratching the tested surface with a diamond indenter with increasing pressure. Furthermore, the gloss of the specimens was determined to evaluate their usefulness in endoscopic work.

Two 3D printers were used to obtain the specimens: a Zortrax M200 Plus FDM printer and a Rapid Shape D20 II printer. The specimens were in the form of a disc with a thickness of 10 [mm] and a diameter of 50 [mm]. The thermoplastic specimens were printed with 100% fill, using a raft as a support material. The diameter of the printer's nozzle chosen to make the parts was 0.4 [mm], with the thickness of the layer of 0.14 [mm]. Extrusion temperatures were 210 [°C] for PLA and 245°C for PETG. The printer's table temperature was 30 [°C] in both cases. Light-cured resin specimens were made with a layer thickness of 50 [µm], without using supporting elements. After the printing process and cleaning of the specimens in an isopropyl alcohol washer, they were further cured using a lamp emitting light with a wavelength of 385 [nm] for the time recommended by the manufacturer.

The technology used to apply the coating is suitable for synthesizing coatings from dielectrics such as Al₂O₃ onto polymeric materials [28]. Al₂O₃ coatings were applied on the printed specimens by pulsed magnetron sputtering with controlled frequency modulation conditions (Fig. 2). Aluminium oxide was synthesized on print surfaces from a circular target with a diameter of 50 [mm] and a thickness of 6 [mm], mounted in a stainless steel vacuum chamber. The vacuum was obtained using a diffusion pump supported by a rotary pump. The target-to-substrate distance was 100 [mm]. The process was carried out in an atmosphere of argon with the addition of oxygen at a constant pressure of 1 [Pa]. The values of the applied powers were 60 [W] at 5 [h] application time and 350 [W] at 1 [h].

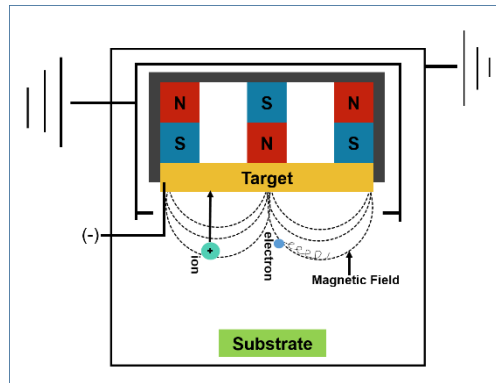


Fig. 2. Diagram of the process of the deposition of the aluminum oxide layer on the specimen surface.

The experimental apparatus used to prepare Al₂O₃ thin films consisted of a multifunctional vacuum chamber equipped with a rotary BL 30 pump and a diffusion SP 800 pump. The vacuum chamber was equipped with a WMK 50 cylindrical magnetron [18], which was powered by a 10 kW DC source with a natural frequency of 100 [kHz] and an adjustable modulating frequency [20, 26]. The vapour source for synthesis was made of 99.99% pure aluminium with a diameter of 50 [mm] and a thickness of 5 [mm]. Based on the previous author's experience [4, 17, 28], the range of parameters used in the study allowed for the reduction in the thermal activity of the substrate. We obtained Al₂O₃ layers on unheated polymer substrates using the pulsed magnetron sputtering [19]. The polymer substrates were placed parallel to the magnetron disk at a distance of 80 mm. The specimens were deposited for 90 and 240 [min]. The power range used was: 80-250 [W], with a modulating frequency of 1000 [Hz]. The process was carried out in a mixture of argon and oxygen. Argon was supplied at a constant pressure of $p_{Ar2} = 1$ [Pa]. Oxygen was added to argon, with the total pressure of $p_{Ar2+O2} = 1.2$ [Pa].

3. Results

2.1. Gloss testing

Macroscopic and microscopic evaluation allowed for the identification of visual changes in the specimens. The deposition of the coating caused a visual change in the specimens for all materials used. The surface acquired a metallic color as shown in Figure 3.

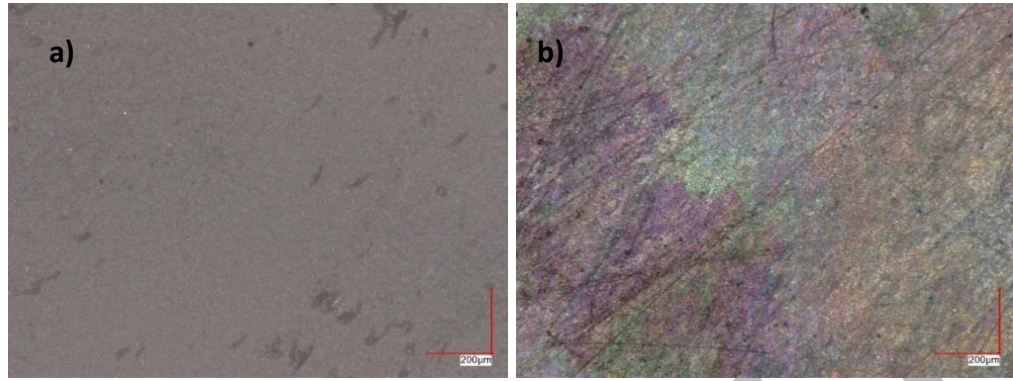


Fig. 3. Diagram of the process of the deposition of the aluminium oxide layer on the specimen surface, a) base sample, b) sample with coating applied.

The seemingly insignificant visual aspect can make a significant difference when introducing plastics into manufacturing practice. In the case of making personalized tools without a coating and with an Al_2O_3 layer applied, as well as accidental "mixing" of the elements, the neurosurgeon can recognize, without much difficulty, whether the tool is coated with a ceramic layer and whether it can be used, for example, for cutting harder tissues such as bone, or whether it is without a layer and can be used only for soft tissues.

Surface gloss was measured using devices called gloss meters. These are devices that emit a stream of unpolarized white light onto a test surface at a specific angle α , and then measure the intensity of the reflected and scattered light over a narrow range of reflection angles. The angle α is determined between a straight line perpendicular to the plane studied and a line parallel to the radiation beam. The results of the measurement are expressed in gloss units (GU). It is assumed that the higher the GU value, the higher the gloss of the tested surface [10, 13, 14].

First, the gloss of commercial neurosurgical instruments made of biometals was tested: (1) specimen 5 - a surgical steel tool, and (2) specimen 6 - a titanium alloy tool. The results obtained were used as baseline measurements and the results of the polymer specimens were related to them because, in modern neurosurgery, metal alloy instruments are mainly used, for which endoscopic work is very cumbersome and difficult due to large light reflections that blind the surgeon during surgery. Surface gloss testing of all specimens was carried out using an Elcometer 406 gloss meter by analyzing three angles of incidence: $\alpha_1 = 20^\circ$, $\alpha_2 = 60^\circ$, and $\alpha_3 = 85^\circ$. Measurements were taken at 4 randomly selected points on the surface of the specimens in accordance with PN-EN ISO 2813 [16]. The results are presented in Table 1.

Table 1. Surface gloss of the tested samples.

Corner			Corner			Corner		
20°	60°	85°	20°	60°	85°	20°	60°	85°
Specimen 1			Specimen 1 + ceramic-coated			Specimen 5		
0,1	2,6	40,4	0,1	2,4	43	136,9	304,4	122,1
0,1	2,2	38,2	0,1	2,1	36,8	133	297,4	113,4
0,1	1,6	38,7	0,1	2,1	39	137	300,5	121,6
0,1	0,9	37,4	0,1	2,2	36,3	137,4	304	121,4
Specimen 2			Specimen 2 + ceramic-coated			Specimen 6		
0,1	2	24	0,1	1,7	27,2	117,8	286,1	78,1
0,1	2,5	25,2	0,1	2,8	30,4	134,9	288,2	79,6
0,1	2,1	20,9	0,1	2	28,2	127,2	287,9	79,6
0,1	2,6	27,7	0,1	1,9	26,4	134,6	286,9	78,2
Specimen 3			Specimen 3 + ceramic-coated					
0,5	11,1	66,8	1,4	17,6	74			
0,6	11,7	68,5	1,5	17,3	71			
0,5	11,1	65,8	1,5	17,9	75			
0,5	11,4	65,3	1,6	17,4	72,8			
Specimen 4			Specimen 4 + ceramic-coated					
0,4	1,1	49,9	0,3	6,7	52			
0,4	1,4	51	0,3	7,2	56,1			
0,4	1,2	51	0,3	6,6	55,1			
0,4	1,2	50,9	0,3	7,3	62,4			

It was found based on the study that polymeric materials have a much lower GU coefficient than metallic materials. The largest differences in terms of beam reflection angle can be observed in the case of the angle of incidence $\alpha_2 = 60^\circ$, where for titanium alloys, the values ranged from $\alpha_{2Ti_min} = 286.1$ GU to $\alpha_{2Ti_max} = 288.2$ GU, while for stainless steel, the minimal and maximal values were $\alpha_{2Steel_min} = 297.4$ GU and $\alpha_{2Steel_max} = 304.4$ GU, respectively. In the case of polymer plastics, these values were disproportionately smaller, and for the plastic characterized by the highest gloss, they reached $\alpha_{2Specimen3_max} = 11.7$ GU, whereas for the remaining materials they were $\alpha_{2Specimen1_max} = 2.6$ GU, $\alpha_{2Specimen2_max} = 2.6$ GU, and $\alpha_{2Specimen4_min} = 1.4$ GU. Deposition of a ceramic layer caused a slight increase of about 7% in the gloss of polymer specimens, although these values were disproportionately lower than the gloss of metallic tools. The smallest differences in beam reflection could be observed between the Ti alloy and the Guide polymer with the coating deposited at an incidence angle of $\alpha = 85^\circ$. The difference in the value was 6% in favour of the ceramic-coated polymer.

2.2. Microscopic and surface topography examinations

The surface topography was assessed using a Keyence VHX-7000 digital microscope. The examinations were performed for baseline specimens (before coating deposition) and those after ceramic coating deposition. Our results highlighted that surface topography was not, it was found that the surface topography does not change and the roughness of the specimen before coating deposition determines the surface topography (Fig. 4-7).

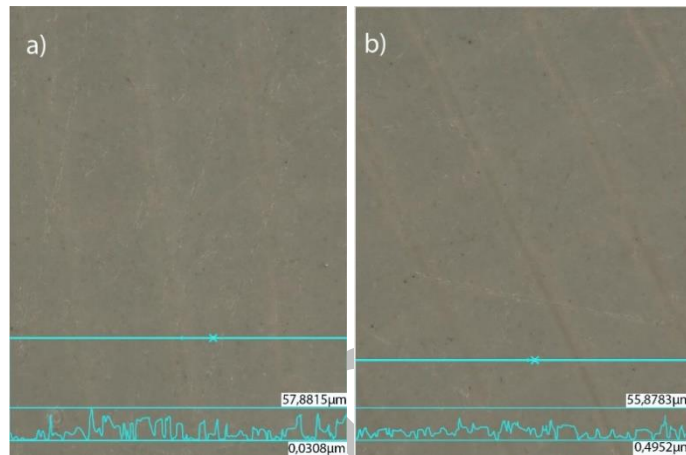


Fig. 4. Surface topography of specimen 1: (a) baseline specimen, b) specimen after deposition of Al_2O_3 coating.

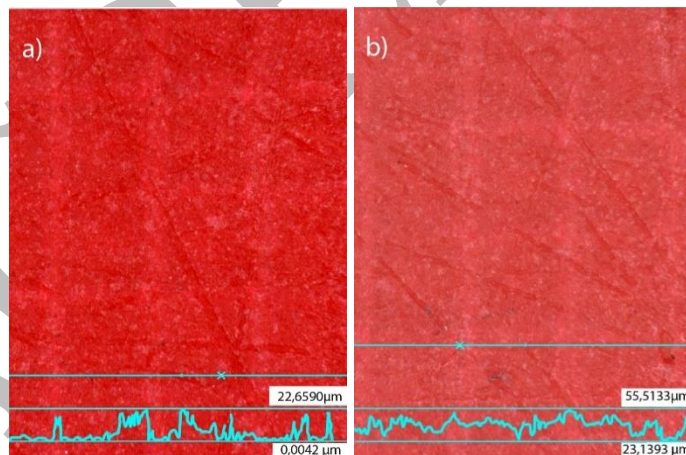


Fig. 5. Surface topography of specimen 2: (a) baseline specimen, b) specimen after deposition of Al_2O_3 coating.

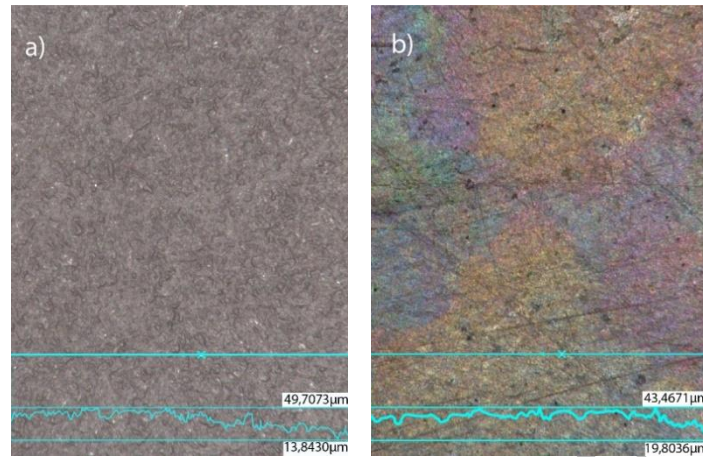


Fig. 6. Surface topography of specimen 3: (a) baseline specimen, b) specimen after deposition of Al_2O_3 coating.

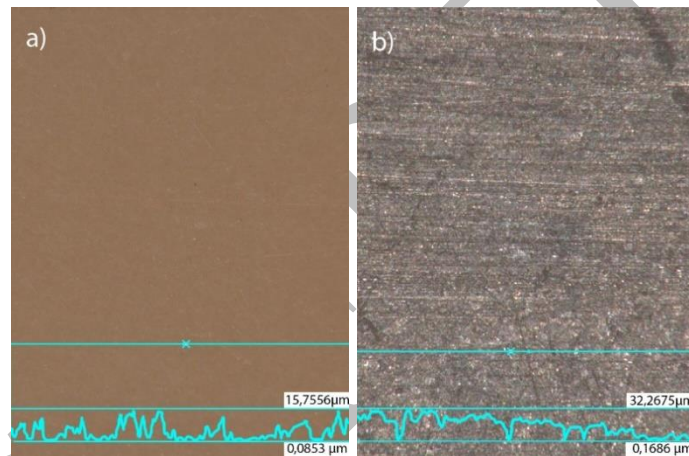


Fig. 7. Surface topography of specimen 4: (a) baseline specimen, b) specimen after deposition of Al_2O_3 coating.

2.3. Evaluation of decohesion of the surface layer

In order to evaluate the mechanical properties of the coatings, we used scratch tester Revetest Xpress CSM Instruments. The examinations allowed for the evaluation of the coating-core system and calculation of the parameters that were essential from the standpoint of function, such as critical decohesion force for the coating, friction force F_t , coefficient of friction, and surface profile.

The test involves scratching the surface with a diamond indenter in the shape of a cone with a radius of $200 \mu\text{m}$, loaded with a normal force F_n . The force applied to the indenter was incremented by 20 N/min , from an initial value of 1 [N] to a final 200 [N] . The indenter speed was 1.51 mm/min .

The total length of a single scratch was 15 mm. During the experiment, the following parameters were determined:

- F_n - normal force diagram,
- F_t - tangential force,
- P_d - indenter penetration depth curve,
- μ - coefficient of friction.

In the case of specimen 1 biopolymer (Fig.8), the resistance to scratching after the deposition of the ceramic coating increased significantly, the decohesion of the material layer and the scratching of the surface in the case of the baseline specimen occurred after reaching 4,5 mm at a decohesion force of $F_n = 58$ N, while after the deposition of the ceramic layer, the indenter moved across the specimen by 33% farther, with a decohesion distance of 6 mm and a decohesion force of $F_n = 72$ N.

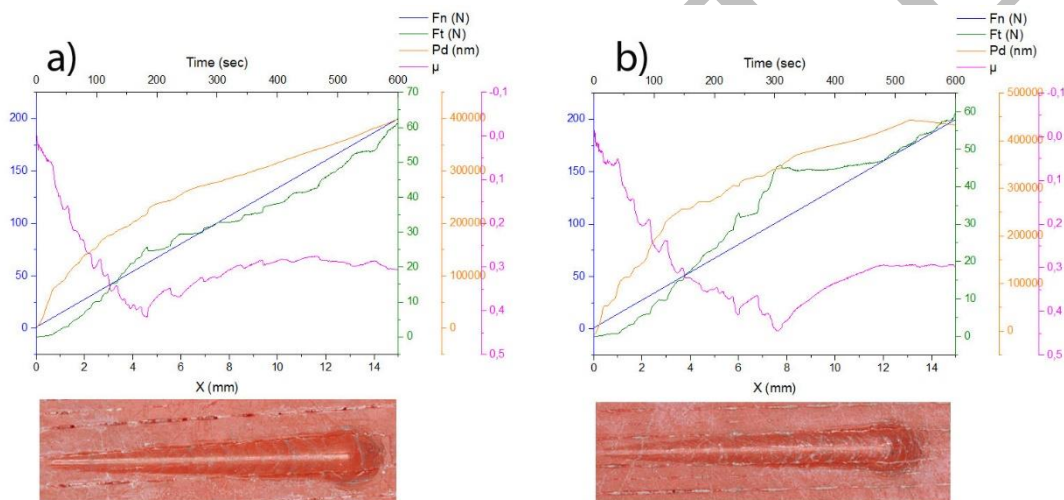


Fig. 8. Scratch test for a specimen 1, (a) baseline specimen, (b) specimen with Al_2O_3 coating.

The largest differences in scratch resistance were noted for specimen 2 (fig. 9). For the baseline material, the scratching of the specimen occurred already after the indenter had traveled 2mm, and the decohesion force was $F_{n_specimen2} = 20$ N. For the same material with the ceramic coating, the decohesion force was $F_{n_specimen2+coated} = 26$ N, which represents a nearly 130% increase in the resistance of the surface layer. Furthermore, the indenter covered a distance of 3 mm, which is 150% of the value of the baseline specimen.

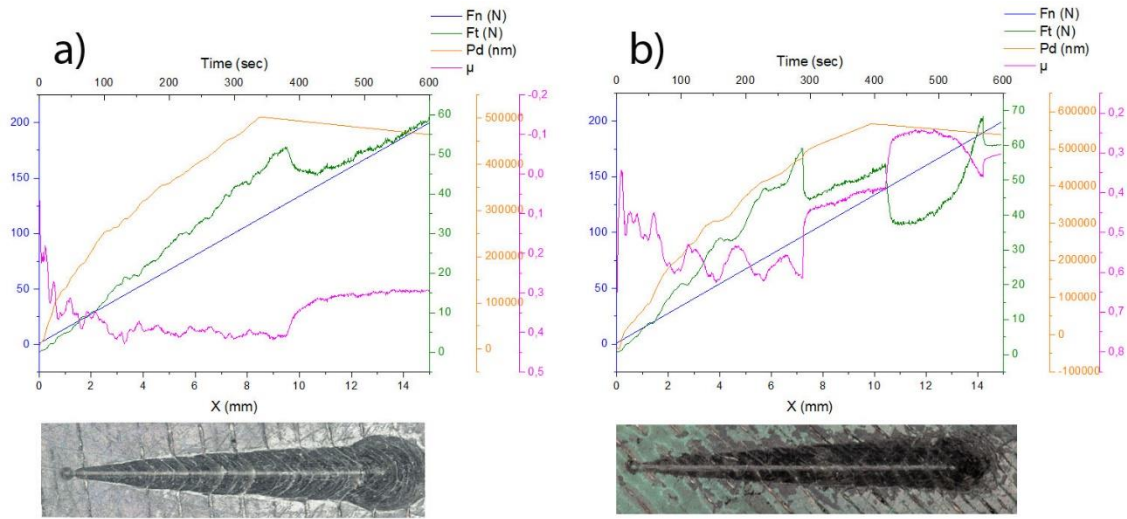


Fig. 9. Scratch test for a specimen 2, (a) baseline specimen, (b) specimen with Al_2O_3 coating.

In the case of specimen 3 biopolymer (Fig.10), the resistance to scratching after the deposition of the ceramic coating increased significantly, the decohesion of the material layer and the scratching of the surface in the case of the baseline specimen occurred after reaching 9.2 mm at a decohesion force of $F_{n_specimen3} = 125 \text{ N}$, while after the deposition of the ceramic layer, the indenter moved across the specimen by 15% farther (a distance of 10.5 mm), at a decohesion force of $F_{n_specimen3+coated} = 133 \text{ N}$. The value of the coefficient of friction remained similar: $\mu_{specimen3} = 0.31$ ($\mu_{specimen3+coated} = 0.34$ for the Al_2O_3 layer).

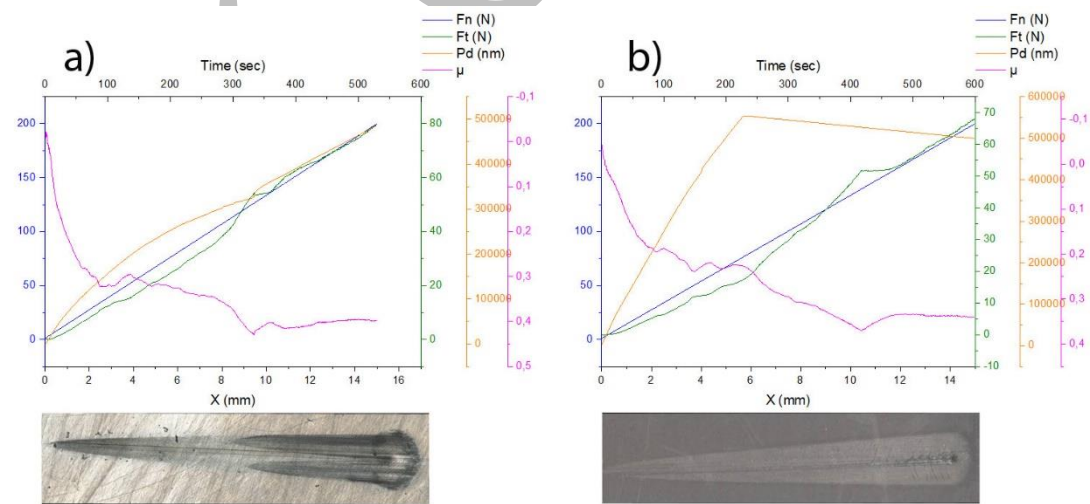


Fig. 10. Scratch test for a specimen 3, (a) baseline specimen, (b) specimen with Al_2O_3 coating.

In the case of the baseline specimen 4 (Fig.11), surface scratching occurred after reaching 3.5 mm at a decohesion force of $F_{n_specimen4} = 50$ N, while after the deposition of the ceramic layer, the indenter moved across the specimen by a distance of 5.8 mm at a decohesion force of $F_{n_specimen4+coated} = 72$ N, accounting for a percentage increase of 44%.

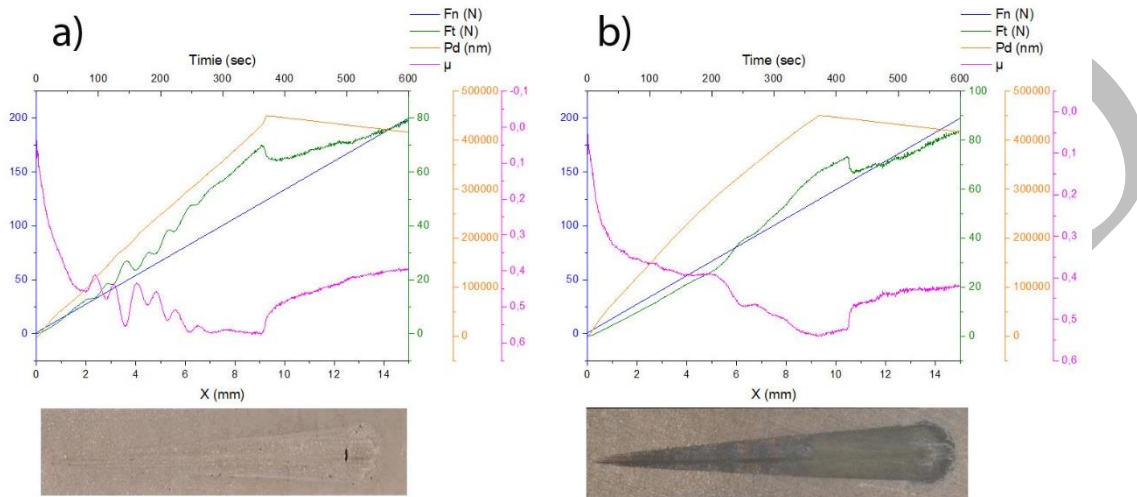


Fig. 11. Scratch test for a specimen 4, (a) baseline specimen, (b) specimen with Al_2O_3 coating.

The values of decohesion forces after coating were significantly higher. Therefore, with the scratch resistance of the tool made of the analyzed materials, it can be used in more responsible works. This parameter is also critical to the durability and reliability of the tool. It offers the possibility of wider application of polymer 3D prints with Al_2O_3 layer in a much wider spectrum than in the case of the baseline material.

4. Discussion

The first attempts to print surgical tools from polymers and their tests performed during simulated operations, according to the literature on the subject, date back to 2013-2016 [1, 7, 11, 12, 13]. The first tools of this type were used in space missions [27]. Since then, there has been significant progress in the quality of the obtained prints, and the use of personalised 3D prints devices are becoming more popular in various medical specialities [6, 23, 27]. The latest trend in surgery and neurosurgery is to adapt tools to the needs and individual characteristics (anatomical, anthropometric, goniometric, etc.) of the patient. The subject of neurosurgical polymer tools is not widely described in scientific publications [2, 24], but industrial applications can be found in the

catalogues of leading global manufacturers. More and more companies introduce disposable medical tools made of polymers, however, although they meet the high requirements of the ISO 10993:1 standard, their durability and reliability are sufficient, but far from the durability and reliability of metal tools. This problem can be reduced by the use of ultra-modern devices that allow covering polymer tools with thin layers with very high strength parameters. The research shows that by coating polymers with Al₂O₃ layers, a significant increase in the wear resistance of the polymer is achieved, surface hardness increases and, consequently, tool wear is reduced. The values of the layer's decohesion forces prove that there is no danger of separating the layer from the substrate, and the ultra-thin layer does not affect the roughness profile of the element, which determines the developed element's ability to be used in exact neurosurgical procedures. Another very important element is the reduction of the gloss of the tools, which in the case of endoscopic operations is crucial for the control and coordination of the tool inside the patient's skull. The next stage of the research will be extensive strength, structural and corrosion tests in a simulated tissue environment as well as instrument sterilization processes. The final stage of the research will be the validation of the process and certification tests.

The use of modern biopolymers to make personalized neurosurgical instruments can be an excellent alternative, especially for individual instruments with complex shapes. It is well known that polymer 3D prints have poor (compared to Ti alloy or stainless steel prints) strength. However, based on experimental studies, 3D prints coated with thin ceramic layers can be an excellent alternative. Deposition of a ceramic layer on polymers significantly improves the mechanical properties of the specimen's surface layer. In the case of material specimen 2, there was an increase of more than 30% in the value of the decohesion force F_n from $F_{n_specimen2} = 20N$ to $F_{n_specimen2+coated} = 26N$. In the case of specimen 1, there was also an increase in the decohesion force of 24% ($F_{n_specimen1+coated} = 58N$ to $F_{n_specimen1+coated} = 72$). The greatest increase in scratch resistance was observed on specimens made of specimen 4, with the values of decohesion force nearly doubled from $F_{n_specimen4} = 50N$ to $F_{n_specimen4+coated} = 72N$.

Preliminary studies confirm that the strength parameters of the materials used are still not fully satisfactory to manufacture a complete tool in the form of a 3D print but they provide ample opportunities to make customized parts for e.g., cutting or delaminating soft tissues from bone, which can be dedicated to a specific patient and cast in a unified handle, thus reducing the need for printing the entire tool to printing the working insert only.

Tests conducted in the present study also indicate the layer's excellent performance in reducing light reflections, which is extremely important for endoscopic work. The polymeric materials used for the pilot study, even under the least favorable lighting conditions, generate a disproportionately low gloss compared to the metallic materials currently in use. Dynamic operation (different angle of incidence of light during surgery), for example, at an angle of incidence of $\alpha=60^{\circ}$ can, in extreme cases, be dramatically less strenuous for the neurosurgeon. Thus, for example, the GU was $\alpha_{2\text{specimen4min}}=297.4$ GU for stainless steel, $\alpha_{2\text{specimen3max}}=11.7$ GU for the polymer material with the highest gloss, while for the other materials it was $\alpha_{2\text{specimen1max}}=2.6\text{GU}$, $\alpha_{2\text{specimen2max}}=2.6\text{GU}$, and $\alpha_{2\text{specimen4min}}=1.4$ GU.

5. Conclusions

Based on the results of the examinations of surface topography, it was found that the primary preparation of the specimen has a decisive effect on the surface roughness. Deposition of a coating does not affect the topography of the surface and it can be assumed that the coated specimen inherits the characteristics of the baseline surface.

Applying an Al_2O_3 layer causes a significant increase in surface strength, which allows us to assume that potentially tools made from such prepared polymers can achieve satisfactory reliability and durability.

The next stage of the research is to carry out strength and microstructural tests allowing for a comprehensive description of the materials. The next stage is to carry out tests on samples after various types of sterilization and after electro-corrosion in an environment simulating body fluids.

Arkadiusz Szarek: the preparation of the research program, the execution of research, the statistical analysis, the interpretation of data, preparation of the manuscript, obtain financing; Justyna Łukomska-Szarek: the statistical analysis, the interpretation of data, preparation of the manuscript, Grzegorz Stradomski: the preparation of the research program, the execution of research, the interpretation of data, Maciej Nadolski: the execution of research, the statistical analysis, Wojciech Wolański: the preparation of the research program, the interpretation of data, Kamil Jozsko: the preparation of the research program, the interpretation of data, Katarzyna Nowakowska-Langier: the execution of research, the interpretation of data, Sebastian Okrasa: the execution of research,

the interpretation of data, Dawid Larysz: the preparation of the research program, the interpretation of data, Patrycja Larysz: the preparation of the research program, the interpretation of data,

References

- [1] Baran E., Erbil H., Baran E.H., Erbil H.Y., Surface modification of 3D printed PLA objects by fused deposition modeling: a review, *Colloids and Interfaces*, 2019, 3, 43, DOI:10.3390/COLLOIDS3020043.
- [2] Boretti A., A perspective on 3D printing in the medical field, *Annals of 3D Printed Medicine*, 2024, February, 13, 100138, <https://doi.org/10.1016/j.stlm.2023.100138>
- [3] Chodun R., Skowronski L., Okrasa S., Wicher B., Nowakowska-Langier K., Zdunek K., Optical TiO₂ layers deposited on polymer substrates by the Gas Injection Magnetron Sputtering technique, *Applied Surface Science*, 2019, 466, <https://doi.org/10.1016/j.apsusc.2018.10.003>
- [4] Culmone C., Smit G., Breedveld P., Additive manufacturing of medical instruments: A state-of-the-art review, *Additive Manufacturing*, 2019, May, 27, 461-473. (2019) <https://doi.org/10.1016/j.addma.2019.03.015>.
- [5] Domingo-Espin M., Puigoriol-Forcada J. M., Garcia-Granada A.A., Llumà J., Borros S., Reyes G., Mechanical property characterization and simulation of fused deposition modeling polycarbonate parts, *Materials & Design*, 2015, 83, 670– 677, <https://doi.org/10.1016/j.matdes.2015.06.074>
- [6] Frizziero L., Santi G.M., Leon-Cardenas Ch., Ferretti., Sali M., Gianese F., Crescentini N., Donnic G., Liverani A., Trisolino G., Zarantonello P., Stallone S., Di Gennaro G.L., Heat Sterilization Effects on Polymeric, FDM-Optimized Orthopedic Cutting Guide for Surgical Procedures, *J. Funct. Biomater*, 2021, 12(4), 63, DOI: 10.3390/jfb12040063.
- [7] George M., Aroom K., Hawes H., Gill B., Love J., 3D Printed Surgical Instruments: The Design and Fabrication Process, *World Journal of Surgery*, 2017, 41(1), 314-319, <https://doi.org/10.1007/s00268-016-3814-5>
- [8] Griffiths C.A., Howarth J., Rowbotham G.A., Rees A., Effect of build parameters on processing efficiency and material performance in fused deposition modelling, *Procedia CIRP*, 2016, 49, 28–32, <https://doi.org/10.1016/j.procir.2015.07.024>

- [9] Hamdi M., Sue H.J., Effect of color, gloss, and surface texture perception on scratch and mar visibility in polymers, *Materials & Design*, 2015, 83, 528-535, DOI: 10.1016/j.matdes.2015.06.073.
- [10] Ignell S., Kleist U., Rigdahl M., Visual perception and measurements of texture and gloss of injection-molded plastics, *Polymer Engineering and Science*, 2009, 49(2), 344-353, <https://doi.org/10.1002/pen.21279>
- [11] Kondor S.A., Grant C.G., Liacouras P.C., Schmid M.J., Parsons L.M., Rastogi V.K., Smith L.S., Macy B., Sabart B., Macedonia, C.R., On Demand Additive Manufacturing of a Basic Surgical Kit. *Journal of Medical Devices-transactions of The Asme*, 2013, 7, 030916, DOI:10.1115/1.4024490
- [12] Kondor S.A., Grant C.G., Liacouras P.C., Schmid M.J., Parsons L.M., Macy B., Sabart B., Macedonia, C.R., Personalized Surgical Instruments, *Journal of Medical Devices-transactions of The Asme*, 2013, 7, 030934, DOI:10.1115/1.4024487
- [13] Landy M.S, A gloss on surface properties, *Nature*, 2007, 447, 158-159, <https://doi.org/10.1038/nature05714>
- [14] Muro-Fraguas, I., Sainz-García, A., López, M., Rojo-Bezares, B., Múgica-Vidal, R., Sainz-García, E., Toledano, P., Sáenz, Y., González-Marcos, A. and Alba-Elías, F., Antibiofilm coatings through atmospheric pressure plasma for 3D printed surgical instruments. *Surface and Coatings Technology*, 2020, 399, 126163, DOI: 10.1016/j.surfcoat.2020.126163
- [15] Okrasa S., Wilczopolska M., Strzelecki G., Nowakowska-Langier K., Chodun R., Minikayev R., Król K., Skowronski L., Namyślak K., Wicher B., Wiraszka A., Zdunek K., The influence of thermal stability on the properties of Cu₃N layers synthesized by pulsed magnetron sputtering method, *Thin Solid Films*, 2021, 735, DOI: 10.1016/j.tsf.2021.138889.
- [16] PN-EN ISO 2813:2001.
- [17] Posadowski W.M., Pulsed magnetron sputtering of reactive compounds, *Thin Solid Films*, 1999, 85–89, 343–344, DOI: 10.1016/S0040-6090(98)01580-6.
- [18] Posadowski W.M., Pulsed magnetron sputtering of reactive compounds, *Thin Solid Films*, 1999, 85, 343–344, DOI: 10.1016/S0040-6090(98)01580-6.
- [19] Posadowski W.M., Wiatrowski A., Dora J., Radzimski Z.J., Magnetron sputtering process control by medium-frequency power supply parameter, *Thin Solid Films*, 2008, 516 (14) 4478, DOI: 10.1016/j.tsf.2007.05.077.

- [20] Redutko J., Kalwik A., Szarek A.: Influence of Curing Time on Properties of Dental Photosensitive Resin Applied in DLP Technique of 3D Printing. *Arch. Metall. Mater.*, 2021, 66(2), 419-424, DOI: 10.24425/amm.2021.135873
- [21] Roy, R. Mukhopadhyay, A., Tribological studies of 3D printed ABS and PLA plastic parts, *Materials Today: Proceedings*, 2021, 41, 856-862, <https://doi.org/10.1016/j.matpr.2020.09.235>
- [22] Shahrubudin N., Koshy P., Alipal J., Kadir M., Lee T., *Heliyon*, 2020, 6(4), p.e 03734, DOI: 10.1016/j.heliyon.2020.e03734.
- [23] Shilo D., Emodi O., Blanc O., Noy D., Rachmiel A.: Printing the future— updates in 3D printing for surgical applications, *Rambam Maimonides Med J*, 2018, 9 (3), DOI:10.5041/RMMJ.10343
- [24] Singh R., Suri, A., Three-Dimensional Printed Ergonomically Improved Microforceps for Microneurosurgery, *World Neurosurgery*, 2020, 141, 271-277, <https://doi.org/10.1016/j.wneu.2020.05.105>
- [25] Strzelecki G.W., Nowakowska-Langier K., Chodun R., Okrasa S., Wicher B., Zdunek K., Influence of modulation frequency on the synthesis of thin films in pulsed magnetron sputtering processes. *Materials Science-Poland*, 2018, 36, 697-703, DOI:10.2478/msp-2018-0078
- [26] Tino R., Moore R., Antoline S., Ravi P., Wake N., Ionita C., Morris J., Decker S., Sheikh A., Rybicki F., COVID-19 and the role of 3D printing in medicine, *3D Print Med*, 2020, 6, 11, DOI: 10.1186/s41205-020-00064-7.
- [27] Wong J.Y., Pfahnl A.C., 3D Printing of Surgical Instruments for Long-Duration Space Missions, *Aviation, Space, and Environmental Medicine*, Aerospace Medical Association, 2014, 85 (7), July, 758-763(6), DOI: 10.3357/ASEM.3898.2014
- [28] Zdunek K., Nowakowska-Langier K., Chodun R., Dora J., Okrasa S., Talik E., Optimization of gas injection conditions during deposition of AlN layers by novel reactive GIMS method” *Materials Science-Poland*. 2014;32(2):171-175. DOI: 10.2478/s13536-013-0169-6.